ACS APPLIED MATERIALS & INTERFACES

Research Article

www.acsami.org

Anisotropic Thermal Diffusivity of Hexagonal Boron Nitride-Filled Polyimide Films: Effects of Filler Particle Size, Aggregation, Orientation, and Polymer Chain Rigidity

Mizuka Tanimoto,[†] Toshitaka Yamagata,[‡] Kenji Miyata,[‡] and Shinji Ando*[,†]

[†]Department of Chemistry and Materials Science, Tokyo Institute of Technology, Ookayama, Meguro-ku, Tokyo 152-8552, Japan

[‡]Electronic Materials Research Department, Shibukawa Plant, Denki Kagaku Kogyo Kabushiki Kaisha, Nakamura, Shibukawa-shi, Gunma 377-8520, Japan

Supporting Information

ABSTRACT: A series of inorganic/organic composite films exhibiting high thermal stability and high thermal diffusivity was prepared from five different grades of flake-shaped hexagonal boron nitride (hBN) and aromatic polyimides (PIs). Thermal diffusivities along the out-of-plane ($D_{\perp}$) and in-plane ($D_{//}$) directions of hBN/PI films were separately measured and analyzed in terms of particle size, shape, concentration, and orientation, as well as molecular structures of rigid and flexible PI matrices. hBN/PI films filled with large flake-shaped particles exhibited a large anisotropy in $D_{\perp}$ and $D_{//}$ due to the strong in-plane orientation of heat-conducting basal plane of hBN, while smaller anisotropy was observed in composites with small flakes and aggregates which tend to orient less in the in-plane direction during film processing. The anisotropic thermal diffusion property observed in hBN/PI films exhibited strong correlation with the orientation of hBN particles estimated using scanning electron micrographs (SEM) and wide-angle X-ray diffraction. Moreover, composites of hBN with a rigid-rod PI matrix exhibited much larger anisotropy in $D_{\perp}$ and $D_{//}$ than flexible PI-composites, reflecting the effect of the rigid and densely packed PI chains preferentially orienting parallel to the film plane. The thermal conductivities of the hBN/rigid-rod PI films were estimated as 5.4 and 17.5 W/m·K along the out-of-plane and in-plane directions, respectively, which is one of the largest values ever reported.

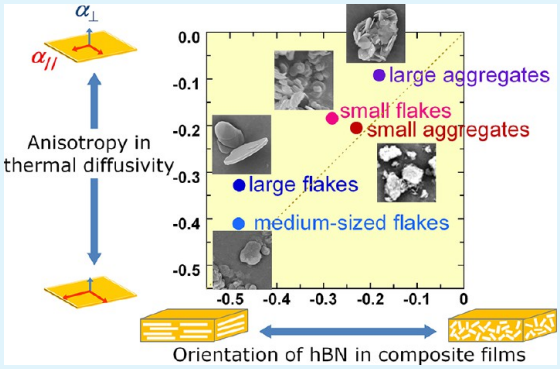

KEYWORDS: *thermal diffusivity, thermal conductivity, polymer−ceramic composite, polyimide, hexagonal boron nitride*

INTRODUCTION

Recent years have seen a tremendous progress in the field of power devices. Despite notable advances in faster and denser circuit technologies, increased heat generation in modern power devices and the resulting difficulty of heat dissipation still remain a challenge. One possible solution is to improve heat dissipation efficiency by enhancing the thermal conductivity (TC, λ) of thermal interface materials (TIMs) used inside the devices. TIMs are polymer-based materials with inorganic particles embedded throughout the matrix in order to overcome the low TCs of polymers. Common TIMs used in electronic devices have been epoxy and silicone based, but TIMs that exhibit higher thermal stability as well as TC are in great demand due to the ever increasing heat generation density and high operating temperature of modern electronic devices.

Polyimides (PIs) are a class of super engineering plastics which are known for their high thermal and chemical stabilities, radiation resistance, and low dielectric constant. These outstanding properties have led to their diverse applications in electronics packaging, such as interlayer dielectric films and substrates for flexible printed circuit boards. These properties also make PIs an ideal candidate for TIM matrices that can resist severer conditions. TC values of PIs, however, are not significantly larger than those of other engineering plastics. It is therefore necessary, in practical applications, to enhance the TC by incorporating inorganic particles.

Despite high industrial needs and a considerable amount of research that has been conducted on PIs, it is only in relatively recent times that the importance of TC of PIs or, more generally, that of polymers has received attention. Although the degrees of TCs of polymeric materials are much smaller both in magnitude and in range compared to metals and ceramics, methods to enhance the TCs of polymers should nevertheless be investigated. According to the Bruggeman approximation,[1] even a small increase of matrix TC has a profound effect on the TC of composites especially at high filler loading. Finite element modeling by Hill and Strader[2] has shown that

Received: February 18, 2013
Accepted: April 22, 2013
Published: April 22, 2013

   dx.doi.org/10.1021/am400615z | ACS Appl. Mater. Interfaces 2013, 5, 4374−4382

increasing the matrix TC from 0.2 to 0.4 W/m·K resulted in a 50% increase in overall composite TC in a 43 vol % hexagonal boron nitride (hBN)/polymer system. The effect of polymeric matrices should therefore not be underestimated.

Aromatic PI films frequently exhibit appreciable anisotropy in physical properties between parallel and perpendicular directions to the film plane. The casting process of PI precursor, poly(amic acid) (PAA), and the subsequent imidization process causes PI chains to orient parallel to the film plane. The degree of orientation varies depending on the molecular structure and processing conditions, giving PIs unique and tunable properties in the in-plane and out-of-plane directions. In-plane thermal diffusivity (TD, $D_{//}$) of Du Pont PI 2556 (3,3′,4,4′-benzophenone tetracarboxylic dianhydride (sBTDA)−4,4′-diaminodiphenylether (ODA)) has been reported to be 4 to 8 times larger than that of out-of-plane thermal diffusivity ($D_{\perp}$).[3] Morikawa et al. reported molecular structure and chain orientation dependences of anisotropic TD of PIs in the in-plane and out-of-plane directions.[4] In addition to the molecular structure and chain orientation, Yorifuji and Ando took into account the degree of molecular packing, as well as more detailed evaluation of structural rigidity/linearity and chain orientation of various PIs in order to further investigate the structure−property relationship.[5] They have reported that among all PIs studied, the highest $D_{\perp}$ values were achieved by PIs exhibiting high chain rigidity and low degree of in-plane orientation. These anisotropic properties of PIs are expected to give rise to differences in $D_{//}$ and $D_{\perp}$ when combined with anisotropic fillers.

Among various inorganic particles, hexagonal boron nitride (hBN)[6] has been recently highlighted due to its potential as a thermal conductive filler material. hBN is a flake-shaped, high aspect ratio synthetic ceramic. It has a crystal structure analogous to graphite, consisting of layers of six-membered rings of alternating, covalently bonded boron and nitrogen atoms stacked and weakly bound by van der Waals forces (Figure 1). Boron atoms in one layer of hexagons are located

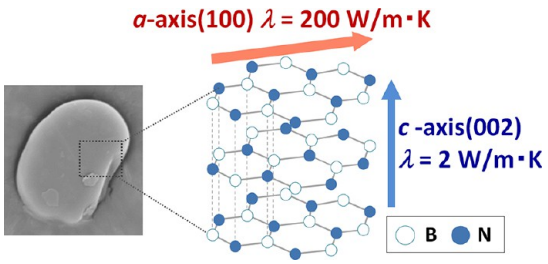

Figure 1. Crystal structure of a typical platelet-shaped hBN particle.

directly over nitrogen atoms in the adjacent layer, whereas in graphite, carbon atoms are located directly below or above the center of six-membered rings in another layer. Anisotropic crystal structure of hBN leads to faster crystal growth in the planar direction and formation of flake-shaped particles exhibiting anisotropic properties. The TC value of hBN is as high as 200 W/m·K in the planar direction, while that in the thickness direction declines to only a few W/m·K.

Sato et al. have recently reported that a high λ value of 7 W/m·K was obtained in a hBN/PI system consisting of subμm sized particles and a thermoplastic PI matrix.[7] Li and Hsu have studied hBN/PI systems with nm- and μm-sized hBN particles and *s*BPDA−ODA PI matrix, and they have shown that mixing nm-sized and μm-sized particles in an optimized ratio effectively enhanced the composite TC.[8]

The significant anisotropies in shape and TC values of hBN are expected to give rise to orientation-dependent TC of composites. Cho and co-workers developed a method to fabricate a polysiloxane/hBN nanosheet composite using a high DC electric field, in which hBN nanosheets are oriented perpendicularly to the film plane.[9] The TC of matrix polysiloxane (0.093 W/m·K) increased to more than 0.14 W/m·K by 5 vol % loading of hBN nanosheets with high degree of orientation in the preferred direction, and the composite TC at the same particle concentration increased as the degree of preferred orientation became higher.

These studies, however, do not cover a wide range of filler loading and different types of hBN particles that come in a variety of sizes and shapes as well as aggregated states, and the focus of these studies has not been on the effect of different polymer matrices. Moreover, although hBN and PIs both have anisotropic properties, thermophysical properties of their composites are often treated as those of an isotropic system or are measured only in one direction.

Another important issue is that the detailed observation of the internal structure of hBN/PI composites is not an easy task because high mechanical strength of PIs makes the composite too tough for the conventional cryofracturing method, and because of their relative softness as ceramics, hBN particles become distorted upon cross-sectioning with blades. The process of cross-sectioning itself distorts the internal structure of hBN/polymer composites. These factors have been a cause of difficulty in obtaining smooth cross sections that allow clear observation of particle orientation as well as formation of voids that affect the composite TC.

This study aims to thoroughly investigate the structure−property relationships of hBN/PI composite films in terms of hBN size, shape, degree of aggregation, and orientation, as well as the structural anisotropy of flexible and rigid PI matrices shown in Figure 2. First, characterizations of hBN/PI

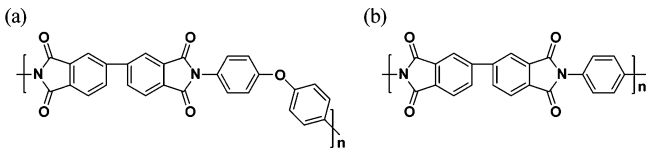

Figure 2. Chemical structures of (a) *s*BPDA−ODA PI (OD) and (b) *s*BPDA−PPD PI (PD).

composite films were performed by estimating the degree of orientation using wide-angle X-ray diffraction (WAXD) measurements and scanning electron micrographs (SEM) of cross sections obtained by a cross section polisher. Thermal diffusion properties were then measured separately for the out-of-plane and in-plane directions, using the temperature wave analysis method and the scanning laser heating AC method, respectively, in order to clarify how these factors affect the in-plane and out-of-plane TD anisotropy of hBN/PI films. As shown in Figure 3, the *z* direction is referred to as "out-of-plane", and the *x* and *y* directions are treated together as "in-plane".

EXPERIMENTAL SECTION

Materials. Five hBN grades having different degrees of aggregation and diameter are shown in Table 1. F(0.7), F(8.0), F(18.0), A(4.0),

dx.doi.org/10.1021/am400615z | ACS Appl. Mater. Interfaces 2013, 5, 4374−4382

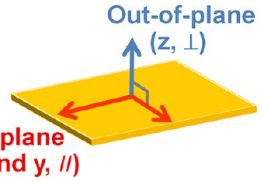

Figure 3. Out-of-plane and in-plane directions of spin-cast films.

Table 1. Grades of hBN Particles with Different Shapes and Sizes

hBN	F(0.7)	F(8.0)	F(18.0)	A(4.0)	A(12.0)
D_{10}(μm)	-	3.2	5.4	0.7	4.3
D_{50}(μm)	0.7	8.0	18.0	4.0	12.0
D_{90}(μm)	-	17.1	41.6	14.2	27.0
Aspect ratio (d/t)	-	22	9	-	-
Particle Shape	flakes			aggregates	

and A(12.0) hBNs were supplied by Denki Kagaku Kougyo K.K. It should be noted that the particle size (D_{50}) refers to the median diameter of the basal plane for flake-type F(0.7), F(8.0), and F(18.0), while for aggregate-type A(4.0) and A(12.0), the value refers to the median diameter of the aggregated secondary particles. Particle size distributions represented by D_{10}, D_{50}, and D_{90} are from the manufacturer's specification sheets. Values for aspect ratios were determined by dividing D_{50} by the average particle thickness measured using SEM images.

3,3′,4,4′-Biphenyltetracarboxylic dianhydride (*s*BPDA) was purchased from Wako Pure Chemical Industries, Ltd. and dried under reduced pressure at 180 °C for 8 h prior to use. 4,4′-Diaminodiphenylether (ODA) and *p*-phenylenediamine (PPD) were purchased from Kanto Chemical co., Inc. and Wako Chemical Industries, Ltd., respectively, and they were purified by sublimation under reduced pressure. *N*,*N*-Dimethylacetamide (DMAc, anhydrous) was purchased from Sigma-Aldrich and used as received.

Preparation of hBN/PI Composite Films. General procedures for preparation of hBN/PI composite films are shown in Figure 4. For comparison between different filler particles, *s*BPDA–ODA PI (OD) films containing 10, 35, 60, and 80 vol % of each of the five hBN particles were prepared. First, hBN-containing slurry was prepared by mixing hBN particles with DMAc. For preparation of slurries containing flake-type F(0.7), F(8.0), and F(18.0), an ultrasonic homogenizer was used to ensure homogeneous dispersion of particles

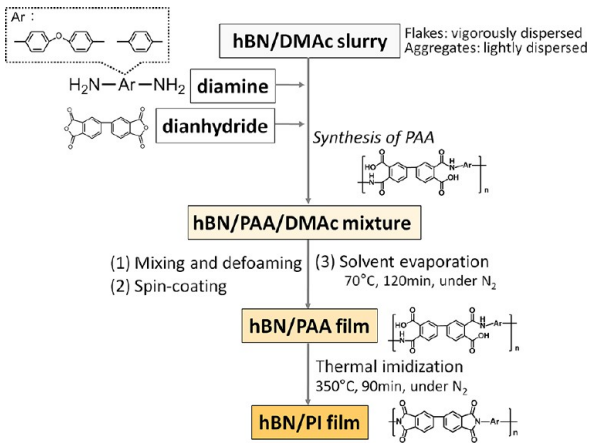

Figure 4. General procedures for preparation of hBN/PI composite films.

in the solvent. Aggregate-type fillers, A(4.0) and A(12.0), were mixed with a magnetic stirrer to prevent fragmentation of aggregates into smaller particles so that the isotropic orientation of primary particles was preserved.

Equimolar amounts of ODA and *s*BPDA were added to the hBN/DMAc slurry in a nitrogen-purged vial and stirred overnight at room temperature until the synthesis of the matrix precursor, poly(amic acid) (PAA), proceeded to completion. The PAA concentration relative to the DMAc was set to 12 wt %. After further mixing and defoaming using a rotation/revolution mixer (Thinky, ARE-310), the hBN/PAA/DMAc mixture was spin-cast on a 4-in. silicon wafer. Prior to imidization, DMAc was evaporated at 70 °C under constant nitrogen flow for 2 h. At the thermal curing step, the hBN/OD-PAA film was heated from 70 to 350 °C at a heating rate of 3.5 °C/min and then finally cured at 350 °C for 90 min to obtain a white-yellow translucent hBN/PI film with film thicknesses of approximately 20 to 50 μm.

For comparison between different PI matrices, flexible *s*BPDA–ODA PI (OD) films and rigid *s*BPDA–PPD PI (PD) films filled with 10, 20, 30, 40, and 50 vol % of F(8.0) particles were prepared by the same procedures. Hereafter, the composite samples will be referred to by the following notation: [volume fraction of hBN particles]v-[grade of hBN]/[type of matrix PI, OD, or PD]. For example, a *s*BPDA–ODA film containing 20 vol % of A(4.0) particles is 20v-A(4.0)/OD.

Characterization of hBN/PI Composite Films. Cross-sectioned samples of hBN/OD films were prepared by argon ion etching using a cross section polisher (JEOL, IB-09020CP) at an accelerating voltage of 6.0 kV. A specimen was covered with a beam-resistant shielding plate. The edge of a hBN/PI specimen was displaced several μm outward of the edge of the shielding plate so that irradiation of Ar ions from above effectively mills the specimen through the thickness direction without causing damage or deformation of internal structures, allowing precise observation of filler dispersion, orientation, and void formation. Micrographs of Au-coated cross sections were obtained using a Hitachi Table Top Microscope (Hitach High-Technologies, TM3000).

Transmission wide-angle X-ray diffraction (WAXD) measurements were performed at BL40B2 beamline, JASRI/SPring-8 (Synchrotron radiation facility, Hyogo, Japan). Peaks corresponding to (100) and (002) reflection were deconvoluted by Gaussian-type functions to obtain the peak intensities $I_{(100)}$ and $I_{(002)}$, which were then used to evaluate the orientation function f by the following equations.

$$f = (1 - K)/(1 + 2K) \quad (1)$$

$$K = k \cdot I_{(100)}/I_{(002)} \quad (2)$$

Here, k is the normalization coefficient determined to be 6.25 by the ratio of relative intensities of $I_{(002)}$ and $I_{(100)}$. The f values describe the degree of the orientation of hBN c-axis relative to the z-axis of the composite film. Complete orientation of hBN c-axis along the out-of-plane and in-plane directions of the composite film gives $f = 1$ and $f = -0.5$, respectively. A random orientation gives $K = 1$ and $f = 0$.

Evaluation of Out-of-Plane and In-Plane Thermal Diffusivity (TD). All thermal diffusivity (TD) measurements were performed at room temperature. Out-of-plane diffusivity ($D_{\perp}$) was measured by the temperature wave analysis (TWA) method (ai-phase Mobile 1u)[10] at an applied voltage of 1.8 V. The $D_{\perp}$ values of film samples were evaluated by a frequency-dependent phase delay of temperature waves. The TD in the in-plane direction ($D_{//}$) was measured by the scanning laser heating AC method (Ulvac-Riko, LaserPIT)[11] at a pulsed frequency of 0.5 Hz. The size of specimens was 25 mm long and 3 mm wide.

RESULTS AND DISCUSSION

Characterization of hBN/OD Films. A simple technique of PI precursor polymerization in hBN-dispersed solvent and a subsequent thermal curing enabled fabrication of hBN/PI films over a wide range of concentrations (Table 2). Most of the hBN/PI films containing 60 vol % filler particles retained

Table 2. Flexibility of hBN/OD Samples[a]

	filler loading (vol %)			
hBN (D_{50}/μm)	10	35	60	80
F(0.7)	++	++	++	+
F(8.0)	++	++	+	+
F(18.0)	++	++	++	+
A(4.0)	++	++	++	−
A(12.0)	++	++	++	−

[a](++) high flexibility; (+) lower flexibility; (−) brittle.

flexibility high enough to resist breakage upon bending and folding as shown in Figure 5, except for 60v-F(8.0)/OD film,

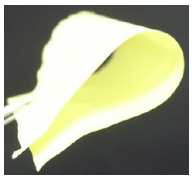

Figure 5. Photograph of 60v-F(18.0)/OD film.

which was bendable but broke apart when folded in half. Although the spin-casting method was applicable to all hBN/PAA solutions up to 80 vol % of hBN concentration, all 80v-hBN/OD films exhibited increased brittleness, making some of them even impossible to be peeled off of the substrates.

SEM Images of Flake hBN-Filled PI Films. *Voids and Defects.* Each flake-shaped hBN/OD sample (Figures 6a−c) showed different patterns of void formation and orientation of hBN particles. As a general trend, no voids were observed at low filler concentrations, though the difference became apparent as the concentration increased.

The amount of voids in 60v-F(8.0)/OD (Figure 6b) was the highest of all samples. Almost no void formation was observed at lower concentration except for a few voids formed underneath or above flat basal hBN planes in 35v-F(8.0)/OD film. On the other hand, voids in 60v-F(8.0)/OD were found near peripheral edges of stacked hBN disks. This is probably the cause of the brittleness of 60v-F(8.0)/OD film (Table 2). In the SEM image of preimidized 60v-F(8.0)/OD-PAA film (Figure 7), almost no voids were observed except for some delamination voids between hBN planes and PI. It can therefore be concluded that these voids formed in the process of condensation reaction and removal of water molecules during thermal curing. Possible factors for the void formation are as follows: (1) There were many interfering layers of hBN before water molecules finally got out of the system, inducing more expanding stress to F(8.0) particles. (2) Once the voids were formed in between building blocks of high-aspect-ratio F(8.0) particles, particles were unable to rearrange and voids were not refilled due to insufficient matrix fluidity. (3) Water molecules generated from PAA in between hBN flat surfaces eventually moved to peripheral edges, where more mobility was attained. It may have also added to increased pressure of gases at hBN peripheral edges.

F(0.7)/OD films (Figure 6a) at all concentrations showed the lowest amount of voids, despite the largest hBN/PI interface area. It is assumed that, during the imidization processes of F(0.7)/OD-PAA films, water molecules were able to get out of the system relatively easily because subμm-sized particles did not interfere with each other. A much fewer number of voids was observed in F(18.0)/OD (Figure 6c) except for some delamination voids. This phenomenon can be attributed to the largest D_{50} and the broadest size distribution, which may have prevented the formation of small building blocks and trapping of water molecules, and to the fact that the number of hBN layers through which the water molecules must pass was less.

Homogeneity of hBN Dispersion. There was no gradient of hBN concentration in the film-thickness direction in F(0.7) and F(8.0) films. The lightweight hBN particles were homogeneously dispersed throughout the film without sinking to the bottom. In 35v-F(18.0)/OD, however, the hBN concentration appears to be higher on the bottom than near the film surface. This inhomogeneity can be attributed to relatively heavy weight of large F(18.0) particles that drew them to the bottom by gravity. At 60 vol %, there was no gradient in particle concentration; the stacking of a high concentration of hBN particles completely filled the system from the bottom to the surface. An increase in the viscosity of PAA solution is expected to improve dispersion in low hBN concentration films.

Orientation of hBN Particles. F(18.0) and F(8.0) particles showed high degree of in-plane orientation at all concentrations. Both the spin-coating process and the thermal imidization process are expected to induce in-plane orientation of hBN flakes by the tensile stress applied along the film plane and the compressive stress applied along the film thickness direction during solvent evaporation and imidization. On the other hand, subμm F(0.7) particles appear to be less affected by these stresses, and they exhibited nearly isotropic orientation. Although F(0.7) particles are flake-shaped, significant in-plane orientation was not induced. It is likely that, because of much smaller D_{50} value relative to the film thickness, F(0.7) particles did not experience high stress forces like large flakes did, and they behaved similarly to isotropic spherical particles.

SEM Images of Aggregated hBN-Filled PI Films. *Voids and Defects.* Most aggregates retained their original structures in A(4.0)/OD and A(12.0)/OD films (Figures 6d,e) although some of them were fragmented into flake-shaped primary particles. Formation of voids was observed at 35 vol % and higher. Almost all of those voids were formed inside the aggregated particles. Apparently, although the film processing condition effectively prevented fragmentation, it also prevented intrinsic pores inside the aggregated particles from being filled by the matrix. Much fewer or no voids were observed around slightly or completely fragmented aggregates. The SEM images also revealed that A(12.0) particles were aggregates of relatively large particles having diameters of more than 10 μm.

Orientation of hBN particles. As shown in Figure 6d,e, nearly isotropic orientation of hBN primary particles was observed in aggregate-filled PI films. The orientation appears to be less isotropic at low concentrations, where the orientation of fragmented primary particles is no longer maintained by other surrounding particles.

Transmission WAXD. As shown in Figure 8, PI films filled with large flake-shaped hBN, F(8.0) and F(18.0), exhibited f values close to −0.5, indicating a high degree of in-plane orientation of the hBN (100) plane. On the other hand, f values of A(12.0)/OD, A(4.0)/OD, and F(0.7)/OD exhibited near-zero values, indicating more isotropic/random orientation of hBN particles. At low concentrations, the f values of A(12.0) and A(4.0) moved away from zero; the contribution of partially fragmented and in-plane-oriented particles is resulting in the f value becoming less. It was shown that f values reflect the shape

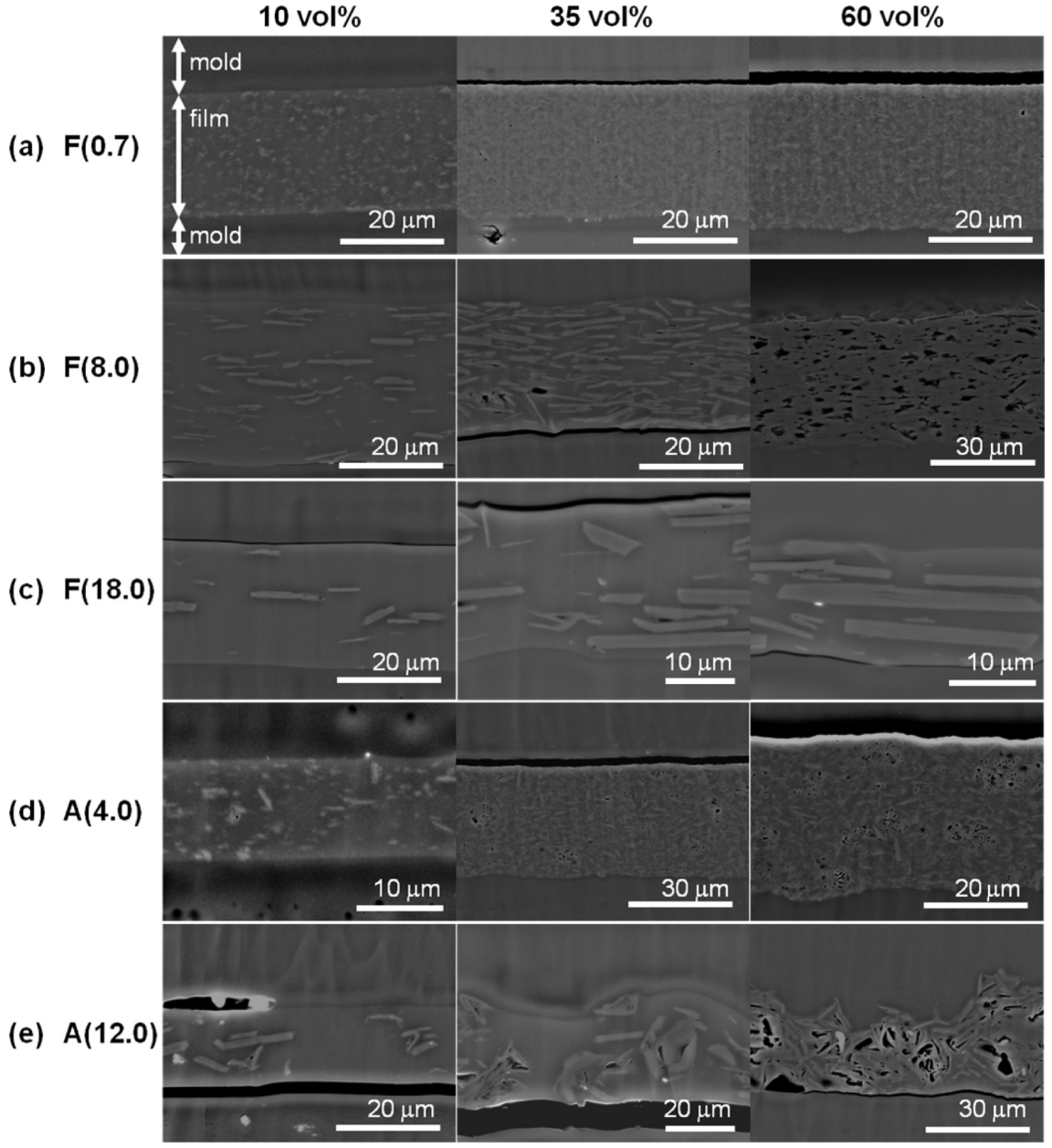

Figure 6. Cross-sectional SEM images of hBN/OD-PI films at 10, 35, and 60 vol % hBN content.

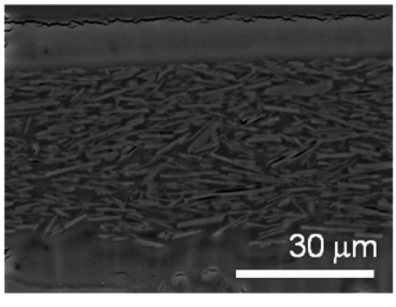

Figure 7. Cross sectional SEM image of 60v-F(8.0)/OD-PAA.

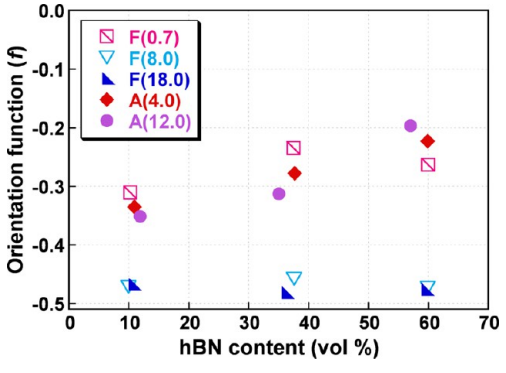

Figure 8. Orientation function (f) of hBN/OD films.

and aggregation state of hBN particles, showing good correlation with the SEM images.

Thermal Transport Properties of hBN/OD Films. *Out-of-Plane Thermal Diffusivity.* As shown in Figure 9a, the $D_{\perp}$ values of hBN films increased up to 60 vol % as the particle concentration increased, regardless of the type of hBN grades. At higher loading of 80 vol %, however, there was only a slight increase in $D_{\perp}$. As mentioned in Characterization of hBN/OD

dx.doi.org/10.1021/am400615z | ACS Appl. Mater. Interfaces 2013, 5, 4374−4382

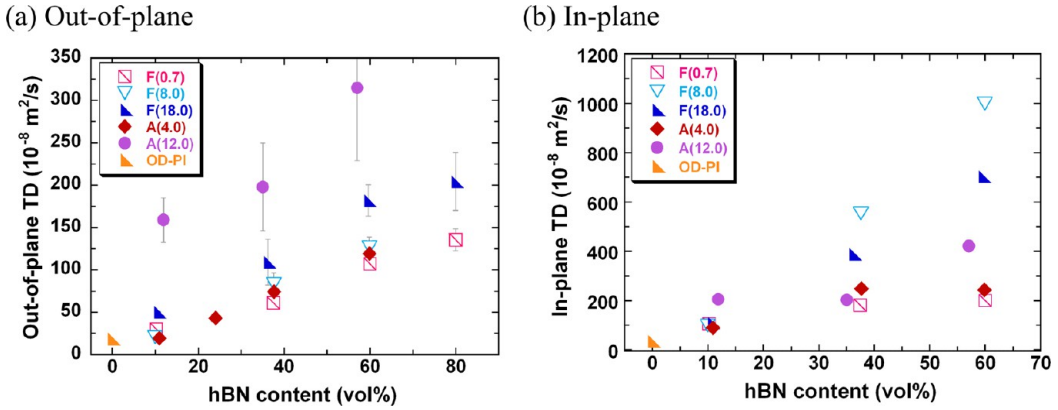

Figure 9. Thermal diffusivities of hBN/OD films. (a) Out-of-plane ($D_{\perp}$) and (b) in-plane ($D_{//}$).

Films, the quality of films significantly deteriorated at 80 vol %. It is assumed that 80 vol % loading exceeds the maximum filler concentration for maintaining the composite structure without any voids or structural deformation. The discontinuity of the matrix caused by voids functioned as effectual thermal insulating layers, which decreased $D_{\perp}$. The same tendency of void formation and decrease in TC has been reported in other hBN/polymer composites.[12] Succeeding discussions from here on will focus on concentrations up to 60 vol %, where the film quality was sufficiently high for various measurements.

The films containing A(12.0) exhibited the highest $D_{\perp}$ at all concentrations. The $D_{\perp}$ at 60 vol % showed approximately a 17-fold increase compared with that of the pristine PI matrix. It is assumed that the highest values of A(12.0)/OD films were achieved by (1) the relatively higher percentage of heat-conducting basal plane oriented in the out-of-plane direction and (2) pathways of strongly aggregated particles that effectively transfer heat to neighboring particles.

Comparison of other hBN/OD films at the same concentrations showed that the $D_{\perp}$ values generally increase as the particle diameter increases. For instance, the $D_{\perp}$ of 60v-hBN/OD film of subμm F(0.7) particles was 107.0×10^{-8} m^2/s, whereas large F(18.0) particle-filled films achieved a $D_{\perp}$ of 181.8×10^{-8} m^2/s at the same concentration. The TD dependence on particle size is believed to be due to the smaller surface area of larger particles and the resulting reduced phonon scattering at the hBN/PI interfaces.

In-Plane Thermal Diffusivity. Figure 9b shows the $D_{//}$ values observed for hBN/OD films with that for pristine OD matrix taken from the literature.[13] The A(12.0)-composites did not exhibit the highest $D_{//}$, whereas the $D_{//}$ values were close to their $D_{\perp}$ values. The small anisotropy in TD reflects the near-isotropic orientation of A(12.0) particles, as was estimated by the WAXD and SEM images. On the other hand, F(18.0)/OD and F(8.0)/OD showed higher in-plane TDs. This result is attributed to smaller interfacial thermal resistance caused by the reduced surface area as well as the higher degree of in-plane orientation of the hBN (100) plane.

Anisotropic Thermal Diffusivity of hBN/OD Films. Figure 10 shows the $D_{\perp}$ and $D_{//}$ values observed for 60v-hBN/OD films. The aggregate-filled films and F(0.7)-filled films are plotted near the dotted line ($D_{\perp} = D_{//}$), indicating small anisotropy in TD. On the other hand, F(18.0) and F(8.0) films show negative deviations from the line, reflecting the much smaller $D_{\perp}$ values with respect to $D_{//}$.

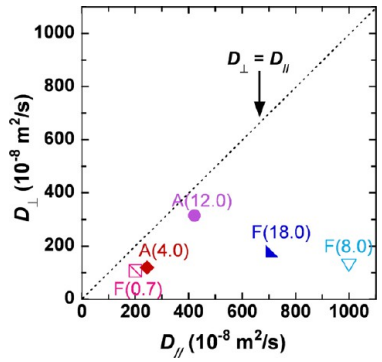

Figure 10. Anisotropy in $D_{\perp}$ and $D_{//}$ of 60v-hBN/OD films.

Figure 11 shows a comparison of the anisotropy in TD with the orientation function *f*. The figure represents the values for

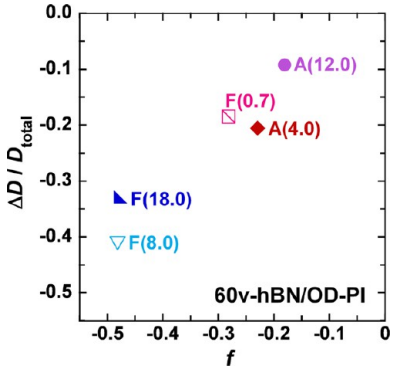

Figure 11. Correlations between orientation function *f* and anisotropy in thermal diffusivity, $\Delta D/D_{total}$.

60v-hBN/OD films. The anisotropy in TD was estimated as $\Delta D/D_{total} = (D_{\perp}-D_{//})/(D_{\perp}+2D_{//})$, in which the denominator D_{total} is the sum of D values in all (x, y, and z) directions. Again, A(12.0), A(4.0), and F(0.7)-films showed values closer to zero in both $\Delta D/D_{total}$ and f, reflecting smaller anisotropy. In contrast, F(18.0) and F(8.0), which showed f values indicating high degree of in-plane orientation of (100) plane, also showed $\Delta D/D_{total}$ values closer to −0.5, confirming a high degree of anisotropy. These correlations agreed well with the SEM images.

Estimation of Thermal Conductivity and Comparison with Models. Thermal conductivity is more commonly used

dx.doi.org/10.1021/am400615z | ACS Appl. Mater. Interfaces 2013, 5, 4374−4382

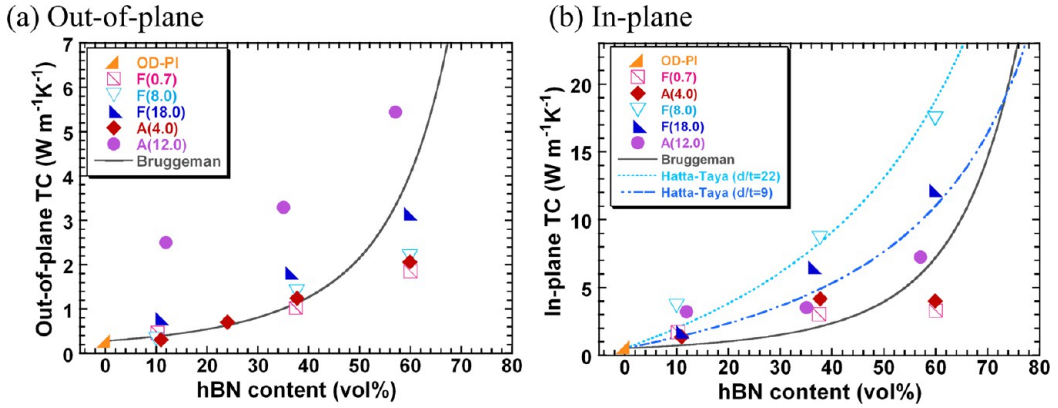

Figure 12. Estimated thermal conductivity of hBN/OD films. (a) Out-of-plane, $\lambda_{\perp}$, and (b) in-plane, $\lambda_{//}$.

Table 3. D, C_p, ρ, and Estimated λ Values of PI Matrices and hBN

	$D_{\perp}$ [10^{-8} m^2/s]	$D_{//}$ [10^{-8} m^2/s]	$\lambda_{\perp}$ [W/m·K]	$\lambda_{//}$ [W/m·K]	ρ [g/cm^3]	C_p [kJ/kg K]
OD-PI	18.3	34.7[a]	0.277	0.526	1.39	1.09
PD-PI	14.9	73.2[a]	0.248	1.22	1.47	1.13
hBN			~2[b]	>200	2.77	0.78

[a]Ref 13. [b]Average $\lambda_{\perp}$ at 300 K, ref 17.

than thermal diffusivity as a property of solid materials' ability to transfer heat. Theoretical models also use thermal conductivity for computation. In order to make a comparison with theoretical models, measured TD values were converted to thermal conductivity λ [W/m·K] by using the relationship in eq 3, where C_p [kJ/kg·K] is the isobaric specific heat and ρ [kg/m^3] is the density. Subscripts c, hBN, and PI represent composite, hBN filler, and PI matrix, respectively. C_{pc} and ρ_c were estimated by the ROM, as shown in eqs 4 and 5. C_p and ρ of hBN and PI are listed in Table 2. C_{pf} and ρ_f were taken from literature,[6] and C_{pPI} and ρ_{PI} were taken from the manufacturer's nominal values for Upilex-RN, which has the same chemical structure as OD-PI.

$$\lambda = D \cdot C_{pc} \cdot \rho_c \tag{3}$$

$$\rho_c = \rho_f \phi + \rho_m (1 - \phi) \tag{4}$$

$$C_{pc} = C_{pf} \phi + C_{pm} (1 - \phi) \tag{5}$$

Estimated out-of-plane and in-plane thermal conductivities, $\lambda_{\perp}$ and $\lambda_{//}$, are shown in Figure 12. The largest values of $\lambda_{\perp}$ and $\lambda_{//}$ were 5.4 and 17.5 W/m·K, respectively. The curve in Figure 12a shows the calculated TC values based on the Bruggeman model,[1] which is a classical model used to predict effective TC of a isotropic system. Measured values for F(0.7)/OD and A(4.0)/OD, both of which contain near-isotropically oriented, relatively small hBN particles, showed good agreement with the prediction up to 35 vol %, with a negative divergence at higher concentration. It is assumed that ideal structure was not achieved at higher concentrations due to imperfect interfaces and voids as was observed in SEM images, and as a result, the measured values became lower than predicted. As for other hBN/OD films, the deviation from the prediction can be explained by large filler sizes which the Bruggeman model does not take into account and by the fact that aggregates form heat-conducting pathways even at low concentrations, making the system inhomogeneous.

Hill and Supancic[14] have compared TCs of ceramic/polymer composites with various theoretical models and have shown that a model called Hatta-Taya model (eq 4)[15] was the most useful in predicting TC values of composites filled with platelet-shaped particles. The measured $D_{//}$ values for F(18.0) and F(8.0) were fit with the Hatta-Taya model, assuming perfect in-plane orientation of the (100) basal plane of hBN. This model takes into account the particle orientation as well as anisotropy in particle shape using a parameter S.

$$\lambda_c = \lambda_{PI} + \frac{\phi(\lambda_{hBN} - \lambda_{PI})\lambda_{PI}}{(\lambda_{hBN} - \lambda_{PI})(1 - \phi)S + \lambda_{PI}} \tag{6}$$

When a matrix contains oblate spheroidal particles, which are oriented parallel (//) or perpendicular ($\perp$) to the direction of heat flow, S can be calculated as follows.

$$S_{\perp} = \frac{x[\cos^{-1} x - x(1 - x^2)]^{1/2}}{2(1 - x^2)^{2/3}} \tag{7}$$

$$S_{//} = 1 - 2S_{\perp} \tag{8}$$

$$x = t/d \tag{9}$$

The variable x in eq 8 is the inverse of the particle aspect ratio. Assuming that flake-shaped hBN particles resemble oblate spheroids having an aspect ratio of diameter d to thickness t and that the longer axes of particles are completely oriented in the in-plane direction, in-plane TC values of F(18.0)/OD and F(8.0)/OD composite films can be estimated. The predicted values are shown in Figure 12b as dotted lines. Although F(18.0) has larger diameter than F(8.0), its aspect ratio is smaller than half of that of F(8.0). It was demonstrated that the Hatta-Taya model fits well with the measured values under these assumptions and that there is a possibility that increasing the filler aspect ratio may lead to significant enhancement of composite TCs.

Effect of PI Matrices on Composite Heat Transport Property. In order to investigate the effect of the rigidity and linearity of matrix PI chains on composite TDs, two types of PI matrices, *s*BPDA–ODA (OD-PI) and *s*BPDA–PPD (PD-PI) were adopted to make composites with F(8.0) hBN particles.

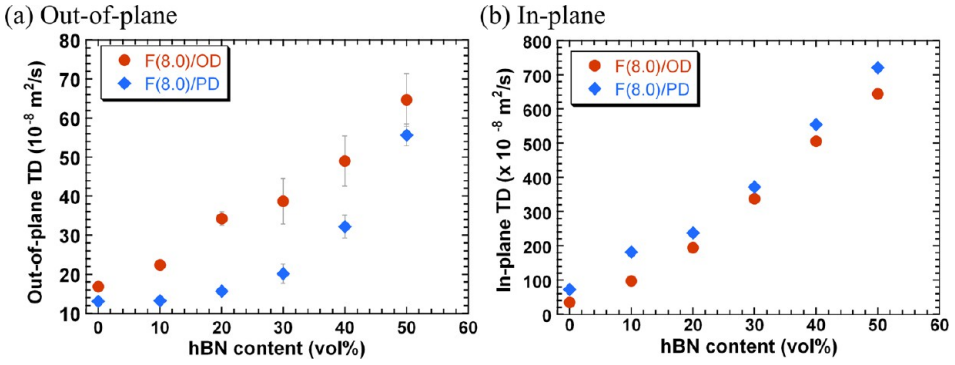

Figure 13. Thermal diffusivity of F(8.0)/OD and F(8.0)/PD films. (a) Out-of-plane ($D_\perp$) and (b) in-plane.

PD-PI has a rigid repeating unit that is known to orient strongly in the film plane. The high degree of in-plane orientation effectively propagates phonons in the in-plane direction. Although both OD-PI and PD-PI are aromatic PIs having relatively rigid repeating units, the orientation of OD-PI chains is known to have small anisotropy due to the flexible diphenylether linkage in the diamine moiety. The in-plane/out-of-plane birefringences of OD-PI and PD-PI films at a wavelength of 1.31 μm were reported as 0.0259 and 0.1697, respectively, which obviously show the strong tendency of in-plane orientation of the latter PI chains.[16] The TD value of OD-PI is less anisotropic than PD-PI. Observed $D_\perp$ and $D_{//}$ values of these two PI matrices are listed in Table 3 along with densities ρ, isobaric specific heat C_p, and in-plane and out-of-plane TCs calculated by eqs 3−5. The $D_\perp$ values of pristine PI matrices were measured in this study, and the $D_{//}$ values were taken from literature.[13] Values for ρ and C_p were taken from manufacturer's nominal values for Upilex-RN and Upilex-S, which have the same chemical structure as OD-PI and PD-PI, respectively.

The measured $D_\perp$ and $D_{//}$ values are plotted in Figure 13a,b, respectively. PD-composites show smaller $D_\perp$ values compared to OD-composites, and a reversed trend was observed in $D_{//}$. The anisotropy in TD is shown in Figure 14. Although both

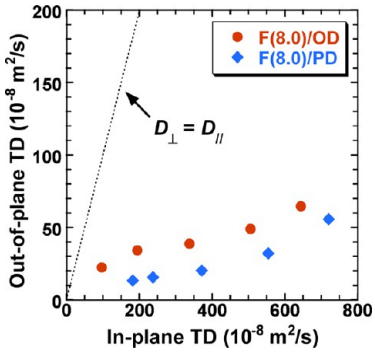

Figure 14. Anisotropy in thermal diffusivity for 10, 20, 30, 40, and 50v-F(8.0)/OD films and F(8.0)/PD films.

OD- and PD-composites showed large anisotropy in the D values, OD-composites were less anisotropic and the data points were slightly closer to the $D_\perp = D_{//}$ line. In addition, the onset of $D_\perp$ increase appeared at higher concentration in PD-composites. It can be attributed to the fact that densely packed PD chains are strongly oriented in the in-plane direction, while OD chains are more randomly oriented and are less densely packed because of the flexible ether linkage which accompanies larger free volumes. Therefore, an addition of only a small volume of hBN particles was not enough to loosen the densely aggregated PD-PI chains. In the in-plane direction, however, the strong in-plane orientation of PD chains effectively enhanced the $D_{//}$ values at all concentrations.

CONCLUSIONS

A series of hBN/PI composite films were prepared by in situ synthesis of PI precursor in a hBN-dispersed solvent and subsequent spin-coating and thermal curing at 350 °C in order to systematically investigate the relationships between out-of-plane (⊥) and in-plane (//) thermal transport properties and the size, shape, volume loading, and orientation of hBN particles, as well as molecular structures of rigid and flexible PI matrices. Measurements of $D_\perp$ and $D_{//}$ values of the composites revealed that flexible OD-PI films filled with large and high-aspect-ratio particles, F(18.0) and F(8.0), exhibited a large anisotropy in TD due to the strong in-plane orientation of heat-conducting basal (100) plane of hBN particles, while smaller anisotropy was observed in films filled with aggregates and small flakes, A(12.0), A(4.0), F(0.7), which are less likely to orient in the in-plane direction during film processing. The TD anisotropy, quantified as $\Delta D/D_{total}$, showed a fairly good agreement with the orientation function f estimated by WAXD; the near-zero $\Delta D/D_{total}$ and values of A(12.0)/OD, A(4.0)/OD, and F(0.7)/OD were consistent with their f values, and both $\Delta D/D_{total}$ and f approached −0.5 in the composite films with large flake shaped F(18.0) and F(8.0) particles. Moreover, composites of hBN and rigid PD-PI matrix exhibited larger TD anisotropy than those of hBN and flexible OD-PI composites, reflecting the effect of the rigid and densely packed PI chains that orient in the in-plane direction. This study clarifies the often-overlooked details of the internal structure of hBN/polymer composites and the structure−property relationship as well as the effects of original particle shapes on composite formation. Since even composite films containing voids marked a high thermal conductivity, the highest $\lambda_{//}$ value being 17.5 W/m·K in the in-plane direction, reduction of voids and improved affinity between hBN particles and the PI matrix are expected to lead to further enhancement of TC in both out-of-plane and in-plane directions.

ASSOCIATED CONTENT

Supporting Information

CTE and TGA thermal analyses of hBN/OD films. This material is available free of charge via the Internet at http://pubs.acs.org.

AUTHOR INFORMATION

Corresponding Author

*Tel: +81-3-5734-2137. Fax: +81-3-5734-2889. E-mail: sando@polymer.titech.ac.jp.

Notes

The authors declare no competing financial interest.

ACKNOWLEDGMENTS

The authors thank Dr. T. Hashimoto and Dr. J. Morikawa of Tokyo Institute of Technology for helpful advice on thermal diffusivity measurements. We would also like to acknowledge Mr. Jun Kouki (Center for Advanced Materials Analysis, Tokyo Institute of Technology) for preparation of cross-section samples and for his valuable suggestions and support. A part of this work was supported by New Energy and Industrial Technology Organization (NEDO). The WAXD experiments were performed with a BL40B2 beamline with the approval of the Japan Synchrotron Radiation Research Institute (JASRI) (Proposal Nos. 2010A-1090, 2011A-1237).

REFERENCES

(1) Bruggeman, D. A. G. *Ann. Phys.* **1936**, *25*, 645−672.
(2) Hill, R. F.; Strader, J. L. *IEEE Trans. Compon., Packag. Technol.* **2007**, *30*, 235−241.
(3) Kurabayashi, K.; Goodson, K. E. *J. Appl. Phys.* **1999**, *86*, 1925−1931.
(4) Morikawa, J.; Hashimoto, T. *J. Appl. Phys.* **2009**, *105*, 113506.
(5) Yorifuji, D.; Ando, S. *Macromolecules* **2010**, *43*, 7583−7593.
(6) Partridge, G. *Adv. Mater.* **1992**, *4*, 51−54.
(7) Sato, K.; Horibe, H.; Shirai, T.; Hotta, Y.; Nakano, H.; Nagai, H.; Mitsuishi, K.; Watari, K. *J. Mater .Chem.* **2010**, *20*, 2749−2752.
(8) Li, T.-L.; Hsu, S.L.-C. *J. Phys. Chem. B* **2010**, *114*, 6825−6829.
(9) Cho, H.-B.; Nakayama, T.; Tokoi, Y.; Endo, S.; Tanaka, S.; Suzuki, T. *Compos. Sci. Technol.* **2010**, *70*, 1681−1686.
(10) Hashimoto, T.; Morikawa, J. *Thermochim. Acta* **1997**, *304/305*, 151−156.
(11) Kato, R.; Maesono, A.; Tye, R. P. *Int. J. Thermophys.* **2001**, *22*, 617−629.
(12) Wang, Z.; Iizuka, T.; Kozako, M.; Ohki, Y.; Tanaka, T. *IEEE Trans. Dielectr. Electr. Insul.* **2011**, *18*, 1963−1972.
(13) Takahashi, F.; Ito, K.; Morikawa, J.; Hashimoto, T.; Hatta, I. *Jpn. J. Appl. Phys.* **2004**, *43*, 7200−7204.
(14) Hill, R. F.; Supancic, P. H. *J. Am. Ceram. Soc.* **2002**, *85*, 851−857.
(15) Hatta, H.; Taya, M. *Int. J. Eng. Sci.* **1986**, *24*, 1159−1172.
(16) Ando, S.; Watanabe, Y.; Matsuura, T. *Jpn. J. Appl. Phys.* **2002**, *41*, 5254−5258.
(17) Simpson, A.; Stuckes, A. D. *J. Phys. C: Solid State Phys.* **1971**, *4*, 1710−1718.